ELSEVIER

Journal of Nuclear Materials 265 (1999) 213–217

journal of nuclear materials

Low cycle fatigue properties and microscopic deformation structure of Zircaloy-4 in recrystallized and stress-relieved conditions

Xiao Lin *, Gu Haicheng

State Key Laboratory for Mechanical Behavior of Materials, Xi'an Jiaotong University, Xi'an 710049, People's Republic of China

Received 31 March 1998; accepted 28 July 1998

Abstract

Low cycle fatigue (LCF) tests have been performed on Zr-4 in recrystallized (RZ) and stress-relieved (SR) conditions at RT and 400°C. Results show that Zr-4/RZ displays cyclic hardening at RT and 400°C, whereas Zr-4/SR exhibits cyclic hardening at RT, but cyclic softening at 400°C. Fatigue lifetime curves as a function of plastic strain range imply that Zr-4/RZ has higher lifetime than that of Zr-4/SR at RT and in the low-cycle region at 400°C, and the LCF properties at 400°C are superior compared to those at RT for Zr-4 in both RZ and SR conditions. TEM examination shows that typical dislocation configuration contains some parallel dislocation lines in Zr-4/RZ, and some dislocation lines are visible between the channels of elongated original grain boundaries for Zr-4/SR at RT. Elongated dislocation cells plus dislocation dipole perpendicular to the cell boundary are observed in Zr-4/RZ, whereas rectangle cells in Zr-4/SR at 400°C. Trace analysis indicates that prismatic and pyramidal slips are possible cyclic deformation modes for Zr-4 in different heat treatment conditions and at different temperatures. Finally, the relationships between LCF properties and microscopic deformation mechanisms are discussed.

1. Introduction

Zircaloy-4 fuel sheathing in pressurized water reactors may be subjected to plastic strain reversal as a result of power fluctuations. Therefore, low cycle fatigue (LCF) properties at room temperature (RT) and the temperature of nuclear reactor operation (375°C) have been obtained for evaluating suitability and safety for use as fuel sheathing. To date, a wealth of LCF data have been obtained for this material [1–4], but limited work has been done on the effect of heat treatment on LCF properties and deformation substructure of Zr-4. The present investigation is intended to provide information on LCF properties and microscopic deformation structure of Zr-4 in different heat treatment conditions to aid in establishing relationships between macroscopic LCF properties and microscopic deformation structures.

2. Experimental procedure

A nuclear-grade of Zr-4 was received in the form of 12 mm diameter cold-worked rods. The chemical composition of the alloy is given in Table 1. Some specimen blanks were subjected a recrystallized treatment of 1 h at 620°C in a vacuum of 10^{-3} Pa, resulting in an equiaxial grain size of approximately 3.5 μm. Others were given to a SR heat treatment of 3 h at 470°C. The LCF specimens with a diameter of 5 mm and a gauge length of 10 mm were machined from these annealed bars. LCF tests were conducted in ambient air on an electro-servohydraulic Mayes machine equipped with a radiant furnace. Symmetric push-pull cyclic loading was employed under strain control at a strain rate of 4×10^{-3} s^{-1} using a triangular waveform. Cyclic load-elongation curves were

* Corresponding author. Fax: 0086 +860-2 932 7910.

0022-3115/99/$ – see front matter
PII: S0022-3115(98)00506-6

Table 1
Chemical composition of Zr-4 (wt%)

Sn	1.4	Pb	<0.0014	Mo	<0.002	Nb	<0.01	H	0.001
Fe	0.23	W	<0.001	Cu	<0.002	Hf	<0.01	O	0.09
Cr	0.1	Co	<0.0014	Si	<0.005	B	<0.00005		
Al	<0.0014	Mn	<0.0014	Cl	<0.002	C	<0.01		
Ti	<0.0014	Mg	<0.0014	V	<0.0014	N	0.003		

recorded periodically on an X–Y plotter. Monotonic tension test was run at the same condition. Thin foils were sectioned perpendicular to the tensile axes, mechanically ground, and electropolished. Dislocation structure was studied with a JEOL-200CX transmission electron microscope (TEM) operated at 200 kV.

3. Results

3.1. Monotonic mechanical properties

Tensile test results are summarized in Table 2, including yield stress (σ_y), ultimate tension strength (σ_b), total elongation (δ), and reduction in area (ψ). σ_y and σ_b decrease as test temperature increases, more than 50% for Zr-4/RZ. At 400°C, Zr-4/SR has good strength and ductility, while Zr-4/RZ shows low strength but high ductility. Based on the static tensile results, it seems that Zr-4/SR has a better combination of strength and ductility than that of Zr-4/RZ at 400°C, which is slightly above the temperature range (340–380°C) designed for nuclear reactor operation.

3.2. Cyclic deformation behavior

Fig. 1 illustrates the cyclic stress–strain curves of Zr-4 in two heat treatment conditions at RT and 400°C, which are obtained by plotting the stress at saturation, σ_a, against the total strain range, $\Delta\varepsilon_t$. For comparison, the corresponding monotonic curves are also included. Fig. 1 shows that both cyclic and monotonic stress-strain curves for Zr-4 at 400°C are much lower than those at RT. Cyclic hardening is displayed for Zr-4 in RZ and SR conditions fatigued at RT by the fact of that the cyclic stress–strain curve lies above the monotonic one. While, at 400°C cyclic softening behavior is displayed for Zr-4/SR, i.e. the cyclic stress-strain curve lies below the monotonic one, yet cyclic hardening is still displayed for Zr-4/RZ. These monotonic and cyclic stress-strain curves of Zr-4 at different heat treatment conditions and testing temperatures can be expressed by the following data in Table 3.

3.3. Fatigue lifetimes

The fatigue lifetime curves as a function of the plastic strain ranges of Zr-4 at the same heat treatment conditions and different testing temperatures are shown in Fig. 2(a) and (b). Generally, Zr-4/RZ has higher LCF lifetime at 400°C than that at RT, specifically at high plastic strain range (Fig. 2(a)). The similar results can be obtained in Zr-4/SR (Fig. 2(b)), but their lifetime difference is more obvious at the lower strain ranges. Fig. 3(a) and (b) display the fatigue lifetime curves of Zr-4 at the same testing temperatures but different heat treatment conditions. The results exhibit that Zr-4/RZ possesses higher fatigue lifetime than that of Zr-4/SR at RT (Fig. 3(a)). However, the fatigue resistance of Zr-4/RZ at 400°C is better compared to Zr-4/SR only in the strain range below 6×10^3 cycles, where two fatigue curves intersect, as shown in Fig. 3(b). The testing results imply that from the view point of LCF performance Zr-4/RZ is superior to Zr-4/SR. Furthermore, the relationship between fatigue lifetime and plastic strain range is presented in Table 4. A power law type relation is obtained.

3.4. Dislocation structure

TEM observation shows that Zr-4 in different heat treatment conditions has different dislocation structure in specimens fatigued at RT and 400°C. Typical dislocation structure of Zr-4 fatigued at RT is shown in Fig. 4(a) and (b). The predominant feature in Zr-4/RZ is dense parallel dislocation lines formed by single slip

Table 2
Uniaxial tensile properties of Zr-4

Heat treatment	Test temperature (°C)	σ_b (MPa)	σ_y (MPa)	δ (%)	ψ (%)
RZ	25	596	419	27	39
	400	277	188	45	59
SR	25	746	530	17	20
	400	443	370	29	39

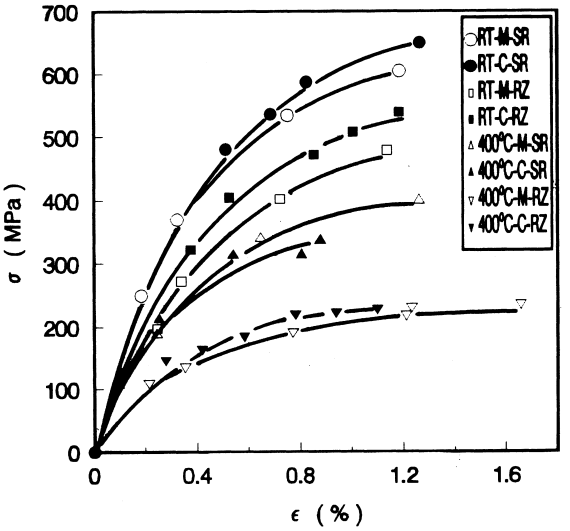

Fig. 1. Monotonic/cyclic stress-strain curves; RZ – Recrystallization; SR – Stress-relief; M – Monotonic; C – Cyclic.

(Fig. 4(a)). Trace analysis indicates that these dislocation lines are formed by prismatic slip [5]. In Zr-4/SR the fatigued dislocation configuration remains the fiber-like grains after warm-extrusion originally. Trace analysis indicates that the elongated grains are seen to be aligned along the pyramidal plane traces, therefore, suggesting that they are produced by the pyramidal slip (Fig. 4(b)) [5–7]. There present some dislocation clusters between the boundaries. On close examination, a lot of edge or screw dislocation segments (labeled with an arrow in Fig. 4(b)) can be observed in the channels between the grain boundaries. Further analysis shows that these dislocation lines are produced by activating prismatic slip during cycling at RT. In comparison with that in Zr-4/SR, the dislocation density in Zr-4/RZ is obviously decreased, and the grains take an equiaxial shape.

Typical dislocation configurations for Zr-4 fatigued at 400°C are shown in Fig. 5. There is a tendency to form rectangular cell structure in both Zr-4/SR and Zr-4/RZ. Typical dislocation structure is elongated subgrain walls aligned with the prismatic plane trace, and dislocation dipoles perpendicular to the prismatic plane trace, i.e., parallel with the pyramidal plane trace, when viewed from the $\{\bar{1}\,2\,\bar{1}\,6\}$ reflection (Fig. 5(a)). From Fig. 5(b), it can be seen that the dislocations arrange in regular rectangular cells in Zr-4/SR fatigued at 400°C. Few dislocations are observed in the interior of these cells. It is noted that some stacking faults appear in the specimens of Zr-4 fatigued at 400°C, as shown in Fig. 5(b) with an arrow.

4. Discussion

The effects of heat treatment and testing temperature on fatigue lifetime of Zr-4 have been studied in the above sections. Zr-4/RZ possesses higher LCF lifetime than that of Zr-4/SR, furthermore, the LCF properties of Zr-4/RZ at 400°C are superior to those at RT. These results imply that Zr-4/RZ has better LCF performance at the operation temperature of reactors, although it has inferior monotonic tensile strength, specifically at 400°C. The reason for this behavior can be qualitatively explained on the basis of the effect of strength and ductility on fatigue lifetime. The higher fatigue lifetime in Zr-4/RZ under strain control LCF testing can be attributed to its higher ductility, since LCF damage is the process of plasticity dissipated. Therefore, a knowledge can be obtained that Zr-4/RZ should be selected preferentially to use as fuel sheathing tubes comparing with Zr-4/SR on the basis of LCF properties and cyclic hardening behavior.

The macroscopic properties are always related with the microscopic deformation structures. In general, increasing the testing temperature will encourage multiplanes slipping, cross slipping and dislocation climbing. The better LCF properties are always related with the higher dispersion of slip systems for hexagonal metals [8,9]. Slip on the first order prismatic planes along $\{1\,0\,\bar{1}\,0\}$ at RT is the common slip system of Zr-4 in two heat treatment conditions, which offers only two independent slip modes [5,10]. The limited plastic deformation ability results in the lower LCF lifetime. The pyramidal slip is considered very important in connection with the ductility of hexagonal Zr-4 at 400°C. From

Table 3
The monotonic/cyclic stress-strain relationships of Zr-4

Heat treatment	Test temperature (°C)	Loading procedure	Regression formulas
RZ	25	Monotonic	$\sigma = 482.11\varepsilon_p^{0.2008}$
		Cyclic	$\Delta\sigma = 575.20\Delta\varepsilon_p^{0.2061}$
	400	Monotonic	$\sigma = 219\varepsilon_p^{0.2181}$
		Cyclic	$\Delta\sigma = 238\Delta\varepsilon_p^{0.2251}$
SR	25	Monotonic	$\sigma = 668.09\varepsilon_p^{0.1513}$
		Cyclic	$\Delta\sigma = 713.72\Delta\varepsilon_p^{0.1187}$
	400	Monotonic	$\sigma = 400\varepsilon_p^{0.0947}$
		Cyclic	$\Delta\sigma = 379\Delta\varepsilon_p^{0.2069}$

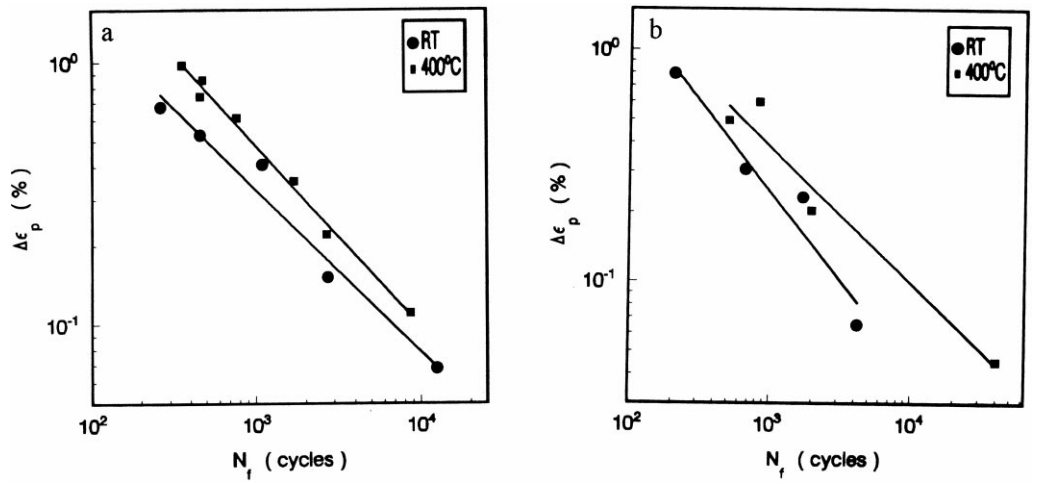

Fig. 2. The relationship curves between plastic strain range and fatigue lifetime for Zr-4 at the same heat treatment conditions and different testing temperatures; (a) Zr-4/RZ; (b) Zr-4/SR.

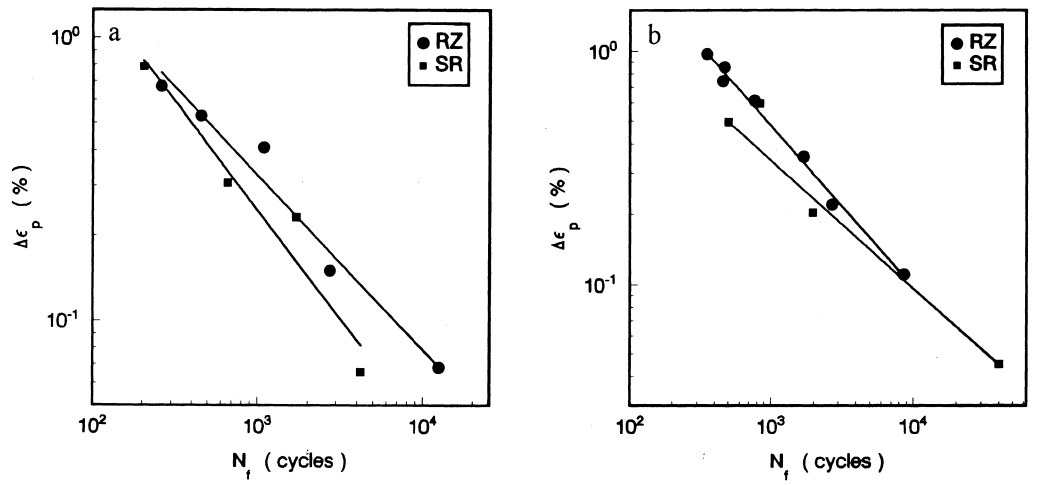

Fig. 3. The relationship curves between plastic strain range and fatigue lifetime for Zr-4 at the same testing temperatures and different heat treatment conditions; (a) RT; (b) 400°C.

Table 4
Application of Coffin-Manson relationship to Zr-4 at different heat treatment conditions and testing temperatures

Heat treatment	Test temperature (°C)	Empirical formulas	Standard deviation	Correlation coefficient
RZ	RT	$\Delta\varepsilon_p N_f^{0.6189} = 23.48$	0.148	0.985
	400	$\Delta\varepsilon_p N_f^{0.6867} = 54.98$	0.067	0.996
SR	RT	$\Delta\varepsilon_p N_f^{0.7667} = 48.97$	0.218	0.970
	400	$\Delta\varepsilon_p N_f^{0.5874} = 22.07$	0.218	0.977

the above section, it is known that there is a tendency of dislocations to form rectangle cells in Zr-4 at both heat treatment conditions fatigued at 400°C. These results would suggest an explanation that the prismatic and pyramidal slips are simultaneously activated at 400°C, which provide five independent slip systems to satisfy von Mises criterion for sustained plastic deformation of polycrystals, so, Zr-4/RZ and Zr-4/SR have excellent ductility at 400°C, and in consequence good LCF performance is achieved.

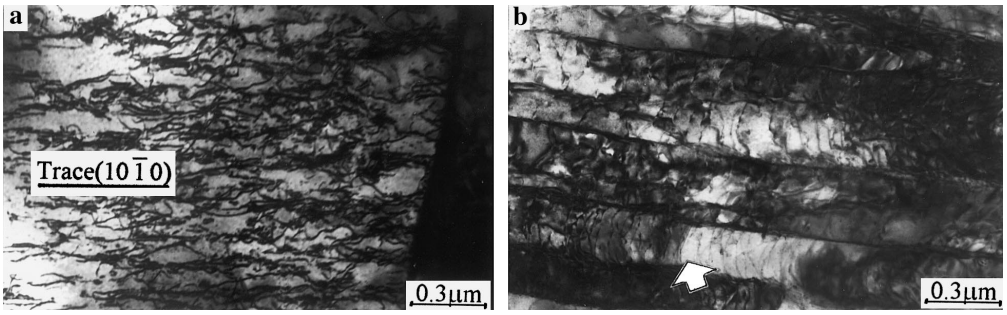

Fig. 4. Typical dislocation configuration of Zr-4 at different heat treatment conditions fatigued at RT; (a) Zr-4/RZ; (b) Zr-4/SR.

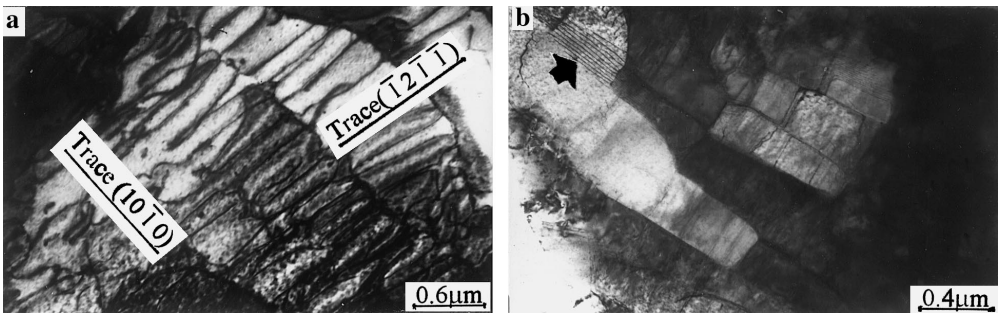

Fig. 5. Typical dislocation configuration of Zr-4 at different heat treatment conditions fatigued at 400°C; (a) Zr-4/RZ; (b) Zr-4/SR.

5. Conclusions

1. Cyclic hardening is exhibited for Zr-4 in both RZ and SR conditions at RT by the fact that the cyclic stress-strain curve lies above monotonic one. Whereas, cyclic softening is displayed in Zr-4/SR, cyclic hardening is displayed in Zr-4/RZ at 400°C.
2. Zr-4/RZ has higher LCF lifetime than that of Zr-4/SR at RT and 400°C, and the LCF properties at 400°C are superior to those at RT in both Zr-4/RZ and Zr-4/SR.
3. Typical dislocation structure is elongated parallel dislocation lines in Zr-4/RZ and a set of curved dislocation lines in Zr-4/SR. There is observed a tendency to form rectangular dislocation cells in both heat treatment conditions at 400°C. The possible plastic deformation modes include: prismatic and pyramidal slip for Zr-4 fatigued at 400°C.

Acknowledgements

The financial support from the National Natural Science Foundation and Nuclear Industrial Science Foundation of China are gratefully acknowledged. We are also grateful for the financial support from the Research Foundation of the State Key Laboratory of Mechanical Structural Strength & Vibration, Xi'an Jiaotong University.

References

[1] P.R. Pandarinathan, P. Vasudevan, J. Nucl. Mater. 91 (1980) 47.
[2] T. Kubo, T. Motomiya, Y. Wakashima, J. Nucl. Mater. 140 (1986) 185.
[3] M. Bocek, I. Alvarez-Armas, A.F. Armas, C. Petersen, Z. Werkstofftech 17 (1986) 317.
[4] A. Beloucif, J. Stolarz, in: G. Lutjering, H. Nowack (Eds.), Fatigue'96, Proceedings of the Sixth International Fatigue Congress, 6–10 May 1996, Berlin, Germany, Elservier, Oxford, 1996, p. 277.
[5] X. Lin, G. Haicheng, Metall. Mater. Trans. 28A (1997) 1021.
[6] X. Lin, G. Haicheng, Chin. J. Aeronaut 9 (1996) 122.
[7] X. Lin, G. Haicheng, K. Zhenbang, Acta Metall. Sinica 8 (1995) 219.
[8] J.G. Grosskreutz, in: S.S. Manson (Eds.), Metal fatigue damage – mechanism, detection, avoidance, and repair with special reference to gas turbine components, ASTM Special Technical Publication, vol. 495, 1971, p. 5.
[9] R.W.K. Honeycombe, The Plastic Deformation of Metals, Edward Arnold, 1984.
[10] M.H. Yoo, Metall. Trans. 12A (1981) 409.